Inorganic Chemistry

Article

pubs.acs.org/IC

Small Molecule Activation Chemistry of Cu−Fe Heterobimetallic Complexes Toward CS_2 and N_2O

Upul Jayarathne, Sean R. Parmelee, and Neal P. Mankad*

Department of Chemistry, University of Illinois at Chicago, 845 W. Taylor Street, Chicago, Illinois 60607, United States

Supporting Information

ABSTRACT: In this contribution, we report the reactivity of polar, unsupported Cu−Fe bonds toward small-molecule heteroallenes. Insertion of CS_2 into the polar Cu−Fe bond of (IMes)Cu-FeCp(CO)$_2$ proceeds at mild conditions and results in the simultaneous presence of two unprecedented CS_2 binding modes (μ_3:η^4 and μ_3:η^3) in the same product. Reactivity between N_2O and (NHC)Cu-FeCp(CO)$_2$ complexes also is observed at mild conditions, resulting in migration of the cyclopentadienyl groups from Fe to Cu. Similar reactivity is observed for new (NHC)Cu-FeCp*(CO)$_2$ analogues, whose structural characterization is reported here and reveals two semibridging Cu···CO interactions per molecule. Stoichiometric oxygen atom transfer from N_2O to PPh_3 was mediated by (IMes)Cu-FeCp(CO)$_2$, indicating the presence of an N_2O-activated intermediate that can be intercepted by exogenous reagents.

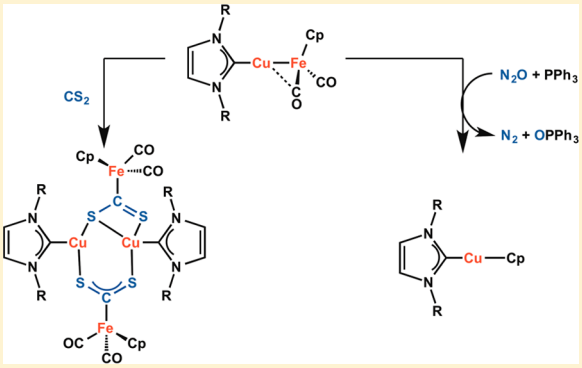

INTRODUCTION

The activation of small molecules such as CO_2 and N_2O is motivated by their role as greenhouse gases, their potential use in commodity chemical synthesis, and the possibility of liquid fuel generation from CO_2.[1] Large kinetic barriers associated with the reactivity of such small-molecule substrates necessitates the use of catalysts, and insight into relevant design strategies is especially valuable if sustainable catalysts composed of earth-abundant elements are to be advanced. In many biological systems, these inert small molecules are activated using a bifunctional approach, wherein acidic and basic sites are occupied by earth-abundant metals that act in cooperation.[2] For example, interconversion of CO and CO_2 occurs using the cooperativity between an acidic Fe site and a basic Ni site in carbon monoxide dehydrogenase (Figure 1a).[3] Similarly, N_2O activation and reduction occur at a tetracopper active site in nitrous oxide reductase.[4] Here, N_2O, which is known to be a notoriously poor ligand for transition metals,[5] is thought to bind to adjacent Cu sites that act cooperatively to activate the small molecule and induce N_2 expulsion (Figure 1b).[6] Similar phenomena are observed in heterogeneous catalysts. For example, N_2O activation by Cu-ZSM-5 is observed only when adjacent Cu sites both are spaced closely enough to cooperatively bind the substrate and are polarized into acidic and basic sites by the zeolite support (Figure 1c).[7] The metal−metal cooperativity inherent to these bioinorganic and heterogeneous small-molecule activation systems motivates the rational design of homogeneous bimetallic systems that can activate small molecules in a productive manner.

Emerging homogeneous systems for cooperative small molecule activation also are comprised of various combinations of metal and/or nonmetal residues. For example, some relevant systems have been fabricated by the pairing of early (acidic site, low d-electron count) and late (basic site, high d-electron count) transition metals,[8] while other pairs feature main group elements in one or both sites (Figure 1d).[9] Despite the fascinating stoichiometric transformations with small molecules exhibited by such bifunctional homogeneous systems, examples of catalytic small molecule activation[2,10] either are prevented by the formation of strong element-heteroatom bonds (e.g., M−O, M−N) featuring early transition metal or main group elements or otherwise require use of stoichiometric O atom acceptors that lessen the utility of the processes.[11] Late transition metals form comparatively labile bonds to heteroatoms but also provide less driving force for small molecule activation to occur. Accordingly, the small molecule activation chemistry of bifunctional systems consisting only of late transition metal pairs is underexplored despite the well-established synthetic protocols for such systems.[12]

In this context, our group has explored the chemistry of (NHC)Cu-Fp complexes (NHC = N-heterocyclic carbene; Fp = FeCp(CO)$_2$), featuring direct Cu−Fe bonds, by pairing together inexpensive and readily available building blocks. These complexes are unusual in that the later, more electronegative, less oxophilic metal serves as the acidic site, and the earlier, more electropositive metal serves as the basic

Received: May 5, 2014
Published: June 30, 2014

   dx.doi.org/10.1021/ic501054z | Inorg. Chem. 2014, 53, 7730−7737

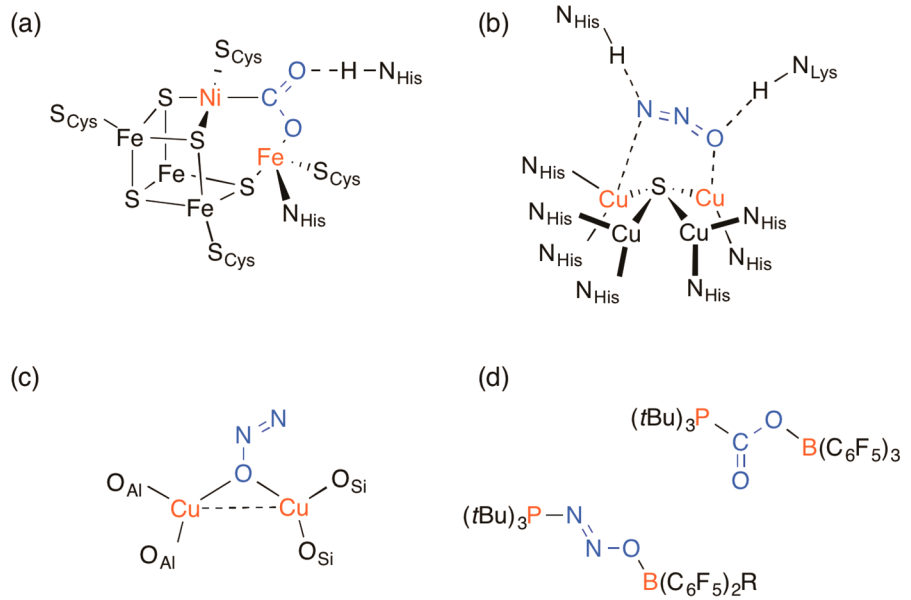

Figure 1. Examples of activation of small molecule substrates (blue) by bifunctional cooperativity (red): (a) CO_2 binding in CODH;[3] (b) proposed N_2O binding in N_2OR;[6] (c) proposed N_2O binding by adjacent Cu sites in Cu-ZSM-5;[7a] (d) CO_2 and N_2O binding by frustrated Lewis pairs.[9b] Cys = cysteine, His = histidine, Lys = lysine, Al = aluminum site, Si = silicon site.

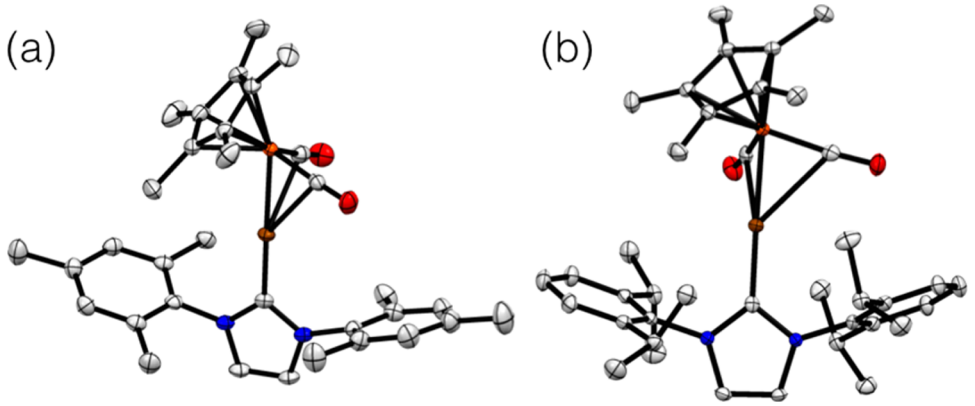

Figure 2. X-ray crystal structures of (NHC)Cu-Fp* complexes (a) **2a** and (b) **2b** plotted as 50% probability ellipsoids. Hydrogen atoms have been omitted for clarity. Atom colors: C, silver; Cu, brown; Fe, orange; N, blue; O, red. Selected bond distances (Å) and angles (deg) for **2a**: Cu−Fe, 2.3215(3); Cu−$C_{carbene}$, 1.889(1); Cu···C_{CO}, 2.408(1) and 2.455(1); $C_{carbene}$−Cu−Fe, 172.95(4); Fe−C−O, 175.9(1) and 176.2(1). For **2b**: Cu−Fe, 2.3414(4); Cu−$C_{carbene}$, 1.908(2); Cu···C_{CO}, 2.521(2) and 2.540(3); $C_{carbene}$−Cu−Fe, 178.88(7); Fe−C−O, 174.4(2) and 174.5(2).

site. This electronic structure view has been validated by experimental and computational methods.[13] Moreover, the potential for these complexes to act as catalysts was demonstrated by our group recently, when we disclosed their utility as base metal catalysts for C−H functionalization.[14] Here we expand the set of Cu−Fe complexes by introducing (NHC)Cu-Fp* analogues (Fp* = $FeCp^*(CO)_2$) and report the reactivity of the complete set of complexes with CS_2, N_2O, and other heteroallene substrates.

RESULTS AND DISCUSSION

Synthesis and Characterization of Fp* Complexes. Previously, we reported the syntheses of (IMes)CuFp (**1a**) and (IPr)CuFp (**1b**) by reactions between (NHC)CuCl synthons and Fp^- (IMes = *N*,*N*′-bis(2,4,6-trimethylphenyl)imidazol-2-ylidene; IPr = *N*,*N*′-bis(2,6-diisopropylphenyl)imidazol-2-ylidene).[13] Analogous preparations were used to synthesize (IMes)CuFp* (**2a**) and (IPr)CuFp* (**2b**) in 65% and 66% yield, respectively (Fp* = $FeCp^*(CO)_2$). Unlike **1a** and **1b**, the new compounds **2a** and **2b** are readily soluble in alkane solvents. Partial formation of the diiron species Fp^*_2 was observed when **2a** and **2b** were stored at room temperature for 1−2 weeks. However, this decomposition could be prevented by storing the complexes in a −35 °C freezer. By contrast, **1a** and **1b** are stable for multiple weeks at room temperature. As expected, the CO vibrational frequencies occur at lower energies for the Fp* complexes compared to the Fp complexes: for example, **2a** (1896, 1823 cm^{-1}) vs **1a** (1905, 1842 cm^{-1}).

Single crystals suitable for X-ray diffraction were obtained by slow evaporation of saturated solutions of **2a** or **2b** in hexane, and both X-ray structures are presented in Figure 2. Surprisingly, little change in Cu−Fe bond distances was observed when comparing **1b** (2.3462(5) Å)[13] and **2b** (2.3414(4) Å) despite the presence of the more sterically demanding Cp* group in **2b**. The Cu−Fe bond distance was even shorter for **2a** (2.3215(3) Å). In fact, only $(Ph_2EtP)_3Fe(\mu\text{-}H)_3Cu(PPh_2Et)$ has achieved a shorter Cu−Fe distance (2.319(1) Å) than that in **2a**.[15] In both **2a** and **2b**, close

dx.doi.org/10.1021/ic501054z | Inorg. Chem. 2014, 53, 7730−7737

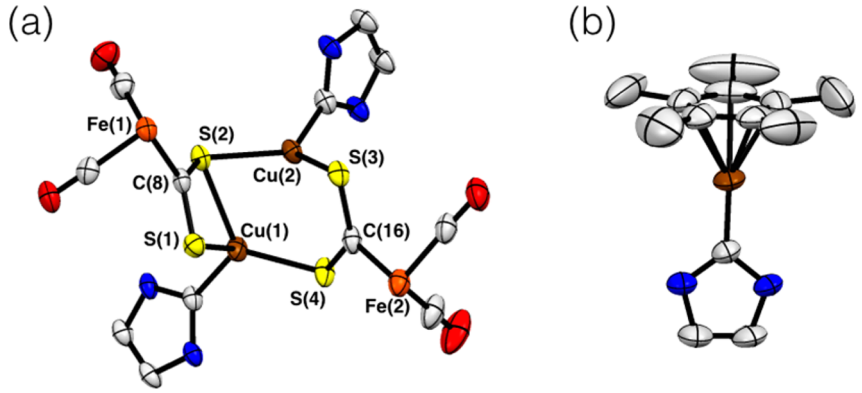

Figure 3. X-ray crystal structures of (a) CS_2 activation product **3** and (b) N_2O activation product **4b** plotted as 50% probability ellipsoids. Nitrogen substituents, cyclopentadienyl groups in **3**, hydrogen atoms, and cocrystallized solvent molecules have been omitted for clarity. Atom colors: C, silver; Cu, brown; Fe, orange; N, blue; O, red; S, yellow. Selected bond distances (Å) and angles (deg) for **3**: Cu(1)···Cu(2), 2.7422(7); Cu(1)−S(1), 2.584(1); Cu(1)−S(2), 2.435(1); Cu(1)−S(4), 2.245(1); Cu(2)−S(2), 2.2621(8); Cu(2)−S(3), 2.290(1); C(8)−S(1), 1.669(4); C(8)−S(2), 1.711(4); C(16)−S(3), 1.690(3); C(16)−S(4), 1.690(3). For **4b**: Cu−$C_{carbene}$, 1.850(3); Cu−$Cp_{centroid}$, 1.871; $C_{carbene}$−Cu−$Cp_{centroid}$, 176.99.

Scheme 1. Reactions with CS_2 and Other Heteroallenes

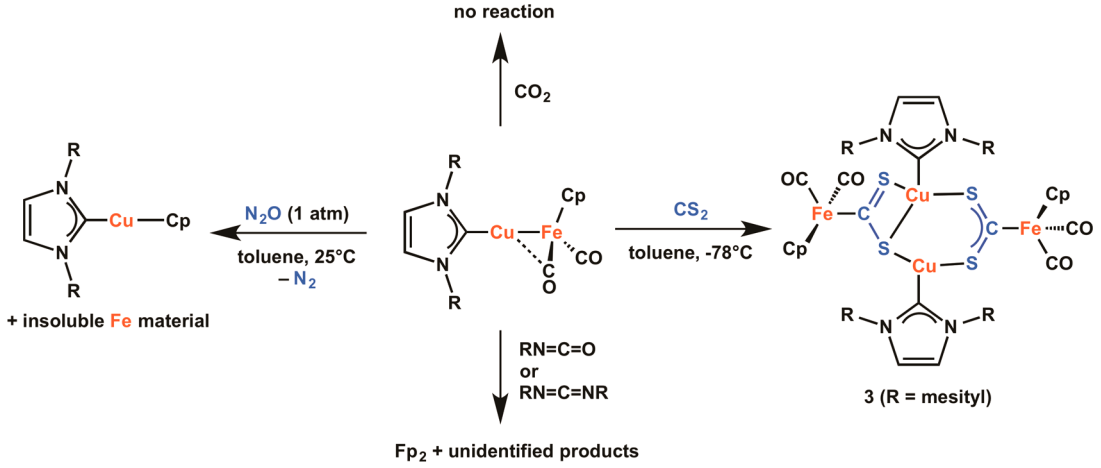

contacts were observed between both CO groups in the Fp* fragment and the electrophilic Cu center. Although the structure of **1b** features such an interaction between the Cu center and only one CO group in the Fp fragment, our previous density functional theory (DFT) calculations of a hypothetical (NHC)Cu-Fp complex predicted the presence of two close Cu···CO contacts.[13] Collectively, these experimental and computational data imply that there is a relatively shallow potential energy surface with regard to these Cu···CO interactions, consistent with our previous assertion of their weak and fluxional nature,[13] and it is likely that crystal packing forces dictate the presence or absence of these interactions in the solid state. The Cu···CO distances are shorter for **1b** (2.423(3) Å) and **2a** (2.408(1) and 2.455(1) Å) than for **2b** (2.521(2) and 2.540(3) Å), reflecting steric congestion around the Cu−Fe core in **2b** created by the bulky IPr and Cp* groups.

Reactivity with CS_2 and Other Heteroallenes. The utilization of CS_2 to model the reactivity of CO_2 has been demonstrated previously, beginning with the first report of a CS_2 complex, $Pt(PPh_3)_2(CS_2)$, in 1966[16] and continuing to more recent studies.[17] Although numerous bimetallic CS_2 adducts are known, the direct insertion of CS_2 into metal−metal bonds is not well precedented.[8b,18b] Instead, the majority of bimetallic CS_2 complexes have been synthesized by reacting CS_2-ligated monometallic fragments with an appropriate second monometallic fragment.[18]

Upon mixing a solution of CS_2 (1 M in toluene) with a yellow-brown solution of **1a** in toluene at −78 °C, a dark red solution resulted. Red, needle-shaped crystals of the product (**3**) were obtained by cooling a concentrated solution in heptane. The solid-state structure of **3** (Figure 3a) features a tetrametallic Cu_2Fe_2 core supported by two bridging CS_2 units having distinct binding modes of μ_3:η^4 and μ_3:η^3. To our knowledge, both binding modes are unprecedented for CS_2. Both binding modes have been observed separately for CO_2,[19] but never in the same molecule. Within the μ_3:η^4-CS_2 ligand, the C(8)−S(2) bond (1.711(4) Å) resembles a C−S single bond and the C(8)−S(1) bond (1.669(4) Å) resembles a C═S double bond, indicating that S(2) behaves as a charge-localized anionic ligand bridging Cu(1) and Cu(2). Within the μ_3:η^3-CS_2 ligand, two equidistant C−S bonds (C(16)−S(3), 1.690(4) Å; C(16)−S(4), 1.690(3) Å) intermediate between C−S single and double bonds suggest anionic charge delocalization across the CS_2 unit. The Cu(1)···Cu(2) distance of 2.7423(7) Å in **3** indicates that Cu···Cu through-space interactions are negligible.

Although the solid-state structure of **3** clearly features two distinct Fp environments, this behavior was not reflected by solution measurements. A single ^{1}H NMR resonance for the two Cp groups was observed in toluene-d_8 to temperatures as

dx.doi.org/10.1021/ic501054z | Inorg. Chem. 2014, 53, 7730−7737

Scheme 2. Oxygen Atom Transfer from N_2O to PPh_3

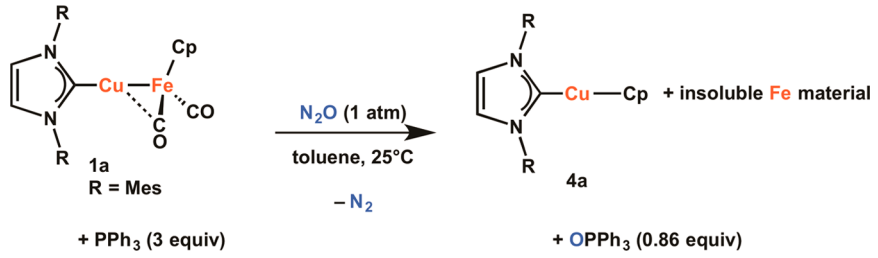

low as −30 °C. Furthermore, only two IR-active CO stretching modes were observed in THF solution (υ_{CO} = 2017, 1967 cm^{-1}) and in powder form (υ_{CO} = 2002, 1950 cm^{-1}). Therefore, at this time we consider the unsymmetrical CS_2 binding in **3** to be a solid-state phenomenon, likely arising from crystal packing forces. Complex **3** is thermally unstable, as significant decomposition was evident by ^1H NMR spectroscopy even after allowing a sample to stand at room temperature for 1 h. Addition of PPh_3 as a sulfur-atom acceptor to **3** did not produce any measurable amount of $SPPh_3$ prior to decomposition.

None of the compounds **1a**, **1b**, **2a**, or **2b** showed reactivity toward CO_2 under the range of conditions we examined in the absence of preactivation by a reductant,[14] making them unusual compared to the many (NHC)Cu-E complexes (E = main group fragment) that insert CO_2 directly under mild conditions.[20] Exposure to $^{13}CO_2$ confirmed that no exchange processes between the carbon dioxide atmosphere and CO ligands within the Fp and Fp* fragments were occurring.[21] Isocyanates (PhNCO, CyNCO) reacted rapidly with **1a** and **1b**, and the carbodiimide ArNCNAr (Ar = *p*-tolyl) reacted rapidly with **1a**, in all cases immediately producing Fp_2 and complicated mixtures of unidentified byproducts (Scheme 1). In none of these cases were heteroallene insertion products detected as reaction intermediates. Although the course of these reactions is unclear, the formation of Fp_2 could indicate oxidation of the heterobimetallic complexes by the heterallene substrates, as Fp_2 also is rapidly produced by reaction of **1a** with the one-electron oxidant, $AgPF_6$.

Reactivity with N_2O. Compared to CS_2 and CO_2, N_2O tends to be a poor ligand for transition metals, as evidenced by the existence of only one structurally characterized complex featuring a terminal N_2O ligand.[5] The favorable thermodynamics of N_2O reactivity generally are suppressed by high kinetic barriers to N_2O activation,[6] motivating research into metal complexes that are capable of N_2O binding. Traditionally, homogeneous systems that exhibit N_2O reactivity feature highly oxophilic or azophilic metal centers that preclude catalytic turnover in many cases.[22] Only recently has bifunctional N_2O activation emerged as an alternative design strategy for homogeneous N_2O activation,[9d,e,23] but again catalysis is precluded by the formation of robust bonds to O and/or N. Because both bioinorganic and heterogeneous systems successfully exploit bimetallic cooperativity involving Cu to activate N_2O (vide supra), it is of note that direct reactions between gaseous N_2O and homogeneous Cu complexes are remarkably rare.[24] In this context, we sought to examine the cooperative activation of N_2O by Cu−Fe heterobimetallic complexes.

Stirring a solution of **1a** in toluene under N_2O (1 atm) at room temperature caused rapid precipitation of a dark brown material. No bands associated with CO, N_2, or N_2O were identified by IR spectroscopy for either the soluble fraction or the precipitate. Analysis of the soluble fraction by ^1H NMR and ^{13}C NMR indicated clean formation of a single product, (IMes)CuCp (**4a**), which has been synthesized previously from (IMes)CuCl and LiCp.[25] The precipitate did not dissolve in any common organic solvents. The X-ray energy dispersive spectrum (see Supporting Information) of this insoluble material indicated the presence of Fe, C, and O as the major constituents, although the exact formula was not established by this method. Solid-state IR spectroscopy of the insoluble material showed strong features in the 1200−1500 cm^{-1} region, which may be indicative of an amorphous iron carbonate material. Analysis of the headspace above the reaction between **1a** and N_2O by GC-MS revealed the stoichiometric formation of N_2, but no evidence for release of either CO or CO_2 was obtained. Complex **1b** behaved similarly upon exposure to N_2O, producing (IPr)CuCp[25] (**4b**) cleanly but at a much slower rate. Complex **2a** also reacted with N_2O, producing (IMes)CuCp* (**4c**) whose connectivity was established by X-ray crystallography (Figure 3b). Similar behavior was observed with **2b** upon exposure to N_2O. The observed Fe-to-Cu migration of Cp (or Cp*) is unique to the heterobimetallic activation of N_2O: exposure of NaFp to N_2O (1 atm) or **1a** to O_2 (1 atm) both resulted in clean formation of Fp_2 with no evidence of Cp dissociation, indicating that all three components (Cu, Fe, and N_2O) are required for the observed transformation.

Exposure of **1a** to N_2O (1 atm) in the presence of PPh_3 (3 equiv) produced $OPPh_3$ (0.86 equiv) along with **4a** (Scheme 2). Once again, only N_2 was detected by GC-MS analysis of the headspace, with no evidence for release of CO and/or CO_2. A material of the same visual appearance and virtually the same IR spectroscopy precipitated from the reaction mixture. The $OPPh_3$ product was not observed when PPh_3 was added to the reaction mixture after N_2O exposure had already occurred. In competition experiments, P(*p*-tolyl)$_3$ outcompeted PPh_3 by a ratio of 2.2:1, and no reaction was observed with P(*o*-tolyl)$_3$, reflecting electronic and steric effects of the O atom transfer reaction, respectively. Because triarylphosphines are unreactive toward both **1a** and N_2O individually under these conditions, these results indicate that a highly oxidizing, electrophilic intermediate forms along the reaction pathway from **1a** to **4a** and can be intercepted by nucleophilic oxygen atom acceptors. It is unlikely that this intermediate is an oxo species such as (IMes)CuOFp, as Fp_2 rather than **4a** was produced when the O atom donor, PhIO, was added to **1a**. Instead, we favor the intermediacy of a bifunctionally activated N_2O adduct that is capable of donating its O atom to PPh_3. Ongoing work in our laboratory involves accessing systems for which such O atom transfer occurs without subsequent Cp migration, which would open the possibility for catalytic oxidation chemistry with N_2O

dx.doi.org/10.1021/ic501054z | Inorg. Chem. 2014, 53, 7730−7737

Table 1. Crystal and Refinement Data for 2a, 2b, 3·0.5C_7H_{16}, and 4c·0.5C_5H_{12}

compound	2a	2b	3·0.5C_7H_{16}	4c·0.5C_5H_{12}
solvent	none	none	heptane	pentane
formula	$C_{33}H_{39}CuFeN_2O_2$	$C_{39}H_{51}CuFeN_2O_2$	$C_{61.5}H_{66}Cu_2Fe_2N_4O_4S_4$	$C_{33.5}H_{45}CuN_2$
fw	615.05	699.21	1292.20	539.26
crystal system	orthorhombic	triclinic	monoclinic	monoclinic
space group	*Pbca*	$P\bar{1}$	$P2_1/n$	$P2_1/n$
color, habit	red plate	red column	red needle	white column
a, Å	16.1443(2)	10.3665(4)	12.0054(3)	8.4518(17)
b, Å	17.4185(3)	11.7857(5)	21.7671(4)	22.254(6)
c, Å	22.8343(3)	16.5689(6)	23.9146(7)	17.184(4)
α, deg	90	84.196(3)	90	90
β, deg	90	82.224(3)	103.279(3)	98.131(7)
γ, deg	90	64.322(4)	90	90
V, Å^3	6421.21(16)	1805.58(12)	6082.4(2)	3199.7(13)
T, K	100.00(10)	100.00(10)	100(2)	300(2)
Z	8	2	4	4
R_1, wR_2	0.0292, 0.0738	0.0379, 0.0859	0.0527, 0.1456	0.0613, 0.1892
GOF	1.036	1.073	1.025	1.074

as a "green" oxidant. Homogeneous catalysts for oxygen atom transfer from N_2O, even using favorable oxygen-atom acceptors such as phosphines, are relatively rare,[26] and the uncatalyzed reaction with PPh_3 requires use of supercritical N_2O as the reaction solvent.[27]

CONCLUSIONS

In summary, the synthesis and crystallographic characterization of two new Cu−Fe heterobimetallic complexes, **2a** and **2b**, and the reactions of such complexes with CS_2 and N_2O are reported here. The structure of CS_2 insertion product **3** shows two new binding modes for CS_2 and a considerable activation of the small molecule. The Cp and Cp* ligands of **1a** and **2a** transfer from Fe to Cu during bimetallic activation of N_2O, and oxygen atom transfer from N_2O to PPh_3 is enabled on a stoichiometric basis from a putative N_2O-activated intermediate. Collectively, these Cu−Fe heterobimetallic complexes display distinct reactivity toward small molecule substrates under mild conditions and show promise for future reaction development.

EXPERIMENTAL SECTION

General Considerations. All reactions and manipulations were conducted under purified N_2 using standard Schlenk line techniques or in a glovebox. Reaction solvents (THF, Toluene, Heptane) were purified using a Glass Contour Solvent System built by Pure Process Technology, LLC. Hexane was purified following the standard procedure.[28] Deuterated solvents (C_6D_6, CD_3CN, toluene-d_8) were degassed by repeated freeze−pump−thaw cycles and stored over activated 3-Å molecular sieves prior to use. ^1H and ^{13}C NMR spectra were recorded using Bruker Avance 400-MHz or 500-MHz spectrometers. NMR spectra were recorded at room temperature, and chemical shifts were referenced to solvent residual peaks; a 20-s recycle delay was used to obtain accurate integration values for Cp hydrogens. FT-IR spectra were recorded in a glovebox using a Bruker ALPHA spectrometer fitted with a diamond-ATR detection unit (for solid samples) or a transmission detection unit (for solution samples). Elemental analyses were performed by Midwest Microlab, LLC, in Indianapolis, IN. Literature procedures were followed in the synthesis of IMes·HCl,[29] IPr·HCl,[29] (NHC)CuCl,[30] Na[Fe(CO)$_2$Cp*],[31] and (NHC)CuFp.[13] N_2O (ultrahigh purity grade) and CS_2 were purchased from commercial sources; CS_2 was degassed prior to use, and N_2O was passed sequentially through activated columns of Drierite (to remove moisture) and GetterMax-133 catalyst tablets (to remove oxygen impurities). Single-crystal X-ray diffraction studies for **2a**, **2b**, and **3** were performed at the X-ray structural lab at Marquette University (Milwaukee, WI). Single-crystal X-ray diffraction studies for **4b** were performed using a Bruker SMART X2S benchtop diffractometer at UIC. Solution and refinement were performed using the SHELX software package by standard techniques.[32] Crystal refinement data are summarized in Table 1. X-ray energy dispersive spectra were collected at the Research Resources Center (RRC) at UIC using a Hitachi S-3000N Variable Pressure SEM with Oxford Inca XEDS system.

Instrumentation for GC-MS Analysis of Headspace. A JEOL GCMate II (JEOL USA, Peabody MA) gas chromatograph/mass spectrometer was used in these experiments. The gas chromatograph was an Agilent 6890Plus (Wilmington DE) equipped with a G1513A autoinjector with 100 vial sample tray connected to a G1512A controller. The gas chromatography column was a fused silica capillary column with a nonpolar 5% phenyl 95% dimethylpolysiloxane phase (Agilent HP-5 ms Ultra Inert), 30 m long, 0.25 mm internal diameter, 0.25 um film thickness. The carrier gas was helium (99.999% Ultra High Purity) run through a STG triple filter (Restek Corp.) at a constant flow rate of 1.2 mL/min. The injector was held at 250 Deg C and was fitted with an Agilent 4 mm ID single taper split liner containing deactivated glass wool. The static headspace analysis was performed using 2 μL of the experimental gas mixture manually injected with a gastight syringe fitted with an isolation valve. The GC inlet split ratio was 20:1. The GC oven was run in isothermal mode at a temperature of 40 °C. Total run time was approximately 6 min. The mass spectrometer was a benchtop magnetic sector operating at a nominal resolving power of 500 using an accelerating voltage of 2500 V. The spectrometer was operated in full scan EI mode (+Ve) with the filament operating at 70 eV scanning from m/z 10 to m/z 850 using a linear magnet scan. The scan speed was 0.2 s/scan. Data analysis was performed using the TSSPro software (Shrader Analytical & Consulting Laboratories, Inc., Detroit MI) provided with the spectrometer. Mass calibration was performed using perfluorokerosene (PFK).

Synthesis of 2a. A round-bottom flask (100 mL) equipped with a stir bar was charged with IMesCuCl (0.209 g, 0.518 mmol) and NaFp* (0.140 g, 0.518 mmol). Upon addition of ∼20 mL of THF, a yellow-brown solution resulted and immediate precipitate formation was observed. This mixture was stirred overnight at room temperature and then filtered through a bed of Celite. The filtrate was evaporated under reduced pressure to obtain a yellow-brown solid. This solid was washed with cold pentane (2 × 3 mL) and dried for 12 h. Yield of **2a**: 0.207 g, 0.336 mmol, 65%. ^1H NMR (C_6D_6, 400 MHz): δ 1.83 (s, 15 H, Cp*), 2.10 (s, 12 H, *o*-CH_3), 2.13 (s, 6 H, *p*-CH_3), 5.97 (s, 2H, NHC), 6.82 (s, 4H, *m*-C<u>H</u>). $^{13}C\{^1H\}$ NMR (C_6D_6, 400 MHz): δ 11.9 (Cp*-(Me)), 17.7 (*o*-CH_3), 21.4 (*p*-CH_3), 90.8 (Cp*), 120.5 (NCH), 129.5 (*m*-C), 135.2 (*o*-C), 136.1 (*ipso*-C), 139.1 (*p*-C), 179.3

dx.doi.org/10.1021/ic501054z | Inorg. Chem. 2014, 53, 7730−7737

(NCCu), 222.7 (CO). IR (Solid, cm^{-1}): 2901, 1896 (ν_{CO}), 1823 (ν_{CO}), 1487, 1377, 1239,1030, 928, 849, Anal. Calcd for $C_{33}H_{39}CuFeN_2O_2$: C, 64.44; H, 6.39; N, 4.55. Found: C, 64.50; H, 6.39 N, 4.58.

Synthesis of 2b. A round-bottom flask (100 mL) equipped with a stir bar was charged with IPrCuCl (0.2622 g, 0.537 mmol), and ∼10 mL of THF was added to it. To this slurry a solution of NaFp* (0.145 g, 0.537 mmol) in THF (10 mL) was added. Immediately, the solution assumed a yellow-brown color with formation of a precipitate. This mixture was stirred overnight at room temperature and then filtered through a bed of Celite. The resulting yellow solution was evaporated to dryness under reduced pressure. Finally, the solid was washed with cold pentane (2 × 5 mL) and dried for 12 h to obtain a fine yellow solid. Yield of **2b**: 0.247 g, 0.353 mmol, 66%. ^{1}H NMR (C_6D_6, 400 MHz): δ 1.09 (d, J = 8.0 Hz, 12 H, CH($C\underline{H}_3$)$_2$), 1.53 (d, J = 8.0 Hz, 12 H, CH($C\underline{H}_3$)$_2$), 1.80 (s, 15 H, Cp*), 2.79 (sept, J = 8.0 Hz, 4 H, C$\underline{H}$(CH$_3$)$_2$), 6.30 (s, 2H, NHC), 7.14 (s, m-C$\underline{H}$, partial overlap with solvent peak), 7.26 (t, J = 8.0 Hz, 2 H, p-C$\underline{H}$). ^{13}C{^{1}H} NMR (C_6D_6, 400 MHz): δ 11.9 (Cp*-(Me)), 24.3 (CH(CH_3)$_2$), 24.4 (CH(CH_3)$_2$), 29.1 (CH(CH_3)$_2$), 90.7 (Cp*), 121.8 (NCH), 124.3 (m-C), 130.4 (p-C), 135.9 (*ipso*-C), 145.8 (o-C), 181.2 (NCCu), 222.9 (CO). IR (solid, cm^{-1}) 2963, 1901 (ν_{CO}), 1842 (ν_{CO}), 1458, 1443, 1381, 1327, 1182, 1031, 769, 736, 660. Anal. Calcd for $C_{39}H_{51}CuFeN_2O_2$: C, 66.99; H, 7.35; N, 4.00. Found: C, 66.80; H, 7.29 N, 4.03.

Synthesis of 3. A solution of **1a** (0.220 g, 0.403 mmol) in toluene (20 mL) was cooled to −78 °C, and then a 1 M solution of CS_2 in toluene (0.524 mL, 0.523 mmol) was added to it. Immediately the solution assumed a reddish color. The stirring continued for 3 h at the same temperature, and then the solvent was evaporated under reduced pressure. The resulting sticky red solid was further dried for 2 h, and a fine red solid obtained. This solid was washed with cold pentane (3 × 3 mL) and further dried for 5h. Yield of **3**: 0.198 g, 79%. ^{1}H NMR (C_6D_6, 400 MHz): δ 2.07 (s, 24 H, o-CH_3), 2.13 (s, 12 H, p-CH_3), 4.22 (s, Cp), 6.05 (s, 4H, NHC), 6.76 (s, 8H, m-C$\underline{H}$). ^{13}C{^{1}H} NMR (toluene-d_8, 500 MHz): δ 17.7 (o-CH_3), 20.95 (p-CH_3), 87.76 (Cp), 120.4 (NCH), 128.9 (m-C), 135.3 (o-C), 136.6 (*ipso*-C), 137.6 (p-C), 214.9 (CO). IR (solid, cm^{-1}): 2002 (ν_{CO}), 1950 (ν_{CO}), 1486, 1432, 1394, 1377, 1310.7, 1263, 1229, 1032, 928, 954, 935, 848, 629, 579, 565. IR (THF, cm^{-1}): 2017 (ν_{CO}), 1967 (ν_{CO}). (Note: The ^{13}C peak for the coordinated CS_2 was not observed. The integration of Cp peak in ^{1}H NMR shows a lower value than expected. This may be due to the unusual relaxation properties of the Cp protons within the Fp fragment, as we have noted previously.[13])

Reaction between N_2O and 1a. Inside the glovebox a 100 mL Schlenk flask equipped with a stir bar was charged with **1a** (0.1871, 0.343 mmol), and toluene (20 mL) was added to it. This flask was connected to a Schlenk line which was under N_2O (1 atm). After approximately 20 min of stirring under N_2O, a precipitate started to form. The stirring was continued overnight at room temperature, and the mixture was filtered through a Schlenk frit. The precipitate was washed with toluene (3 × 3 mL). The filtrate was evaporated under reduced pressure to obtained IMesCuCp as a light yellow solid. Yield of **4a**: 0.107g, 72%. ^{1}H NMR (C_6D_6, 400 MHz): δ 1.97 (s, 12 H, o-CH_3), 2.12 (s, 6 H, p-CH_3), 5.91 (s, 5H, Cp), 6.04 (s, 2H, NCH), 6.77 (s, 4H, m-CH). ^{13}C{^{1}H} NMR (C_6D_6, 400 MHz): δ 17.8 (o-CH_3), 21.0 (p-CH_3), 95.0 (Cp), 120.8 (NCH), 129.1 (m-C), 135.2(o-C), 136.9(*ipso*-C), 138.6(p-C). The precipitate formed initially during the reaction was recovered from the Schlenk frit and analyzed by X-ray energy dispersive spectroscopy, yielding the spectrum shown in Supporting Information.

Headspace Analysis of Reaction between N_2O and ***1a.*** A Schlenk flask with a stir bar was charged with **1a** (0.100 g, 0.183 mmol) and THF (56 mL) under an atmosphere of nitrogen, producing a yellow solution with a headspace volume approximately equal to 5 equiv of gas, assuming ideal behavior at 298 K. The flask was sealed with a rubber septum. Three freeze−pump−thaw cycles were performed, after which the solution was allowed to warm to room temperature. Exposure of this solution to N_2O, with vigorous stirring, caused the formation of a brown precipitate. The mixture was allowed to stir for a total of 4 h. Mass spectra of the N_2O reagent gas and the headspace after the reaction were obtained via 2 μL injections at 40 °C.

Reaction between N_2O and 2a. A 100 mL Schlenk flask containing a toluene (20 mL) solution of **2a** (0.1987 g, 0.323 mmol) was exposed to N_2O gas (1 atm). Effervescence was observed at the beginning, and the solution became dark brown in color after 0.5 h of stirring. After stirring for an additional 2.5 h, the mixture was filtered through a Schlenk frit, and the precipitate was washed with toluene (2 × 5 mL). Evaporating the filtrate to dryness yielded a light brown solid. ^{1}H NMR analysis of this solid indicated the formation of **4c** and Fp*$_2$, the latter of which forms at some rate from thermal decomposition of **2a**. Cooling a concentrated pentane solution of this mixture yielded colorless crystals of **4c**. The conversion to **4c** was determined separately by ^{1}H NMR using 2,4,6-trimethoxybenzene as an internal standard: 38%. Spectral data for **4c** matched those obtained from independent synthesis from (IMes)CuCl and LiCp*, as did unit cell parameters determined by submitting the crystals to X-ray diffraction.

Independent Synthesis of 4c. Inside the glovebox a 50 mL round-bottom flask equipped with a stir bar was charged with pentamethylcyclopentadiene (0.061 g, 0.447 mmol), and THF (10 mL) was added to it. This flask then was placed in a cold well that had been prechilled to −78 °C, and a solution of n-butyllithium (1.6 M in hexanes, 0.279 mL, 0.447 mmol) was added to it. The flask was then taken out of the cold well and stirred at room temperature for 3 h, during which time a white slurry was resulted. To this slurry IMesCuCl (0.180 g, 0.447 mmol) was transferred using THF (5 mL), and the resulting mixture was stirred overnight. The solution was then filtered through a bed of Celite, and filtrate was evaporated under reduced pressure to obtain **4c** as a spectroscopically pure white solid. Yield: 0.202 g, 90%. ^{1}H NMR (C_6D_6, 400 MHz): δ 1.96 (s, 12H, o-CH_3), 2.07 (s, 15H, Cp*-CH_3), 2.18 (s, 6H, p-CH_3), 6.02 (s, 2H, NCH), 6.83 (s, 4H, m-CH). ^{13}C{^{1}H} NMR (benzene-d_6, 400 MHz): δ 11.0 (Cp*-CH_3) 17.3 (o-CH_3), 20.7 (p-CH_3), 99.7 (Cp*), 119.9 (NCH), 128.8 (m-C), 135.1(o-C),136.8 (*ipso*-C), 138.1(p-C), 188.4 (NCN). Anal. Calcd for $C_{31}H_{39}N_2Cu$: C, 73.99; H, 7.81; N, 5.57. Found: C, 73.49; H, 7.55; N, 5.06. Crystals suitable for X-ray diffraction were obtained by cooling a concentrated pentane solution of **4c** to −33 °C.

Reaction between N_2O and 1a in the Presence of PPh_3. A Schlenk flask with a stir bar was charged with **1a** (0.100 g, 0.183 mmol), triphenylphosphine (0.144 g, 0.549 mmol), and THF (15 mL) under an atmosphere of nitrogen, producing an orange solution. Three freeze−pump−thaw cycles were performed, after which the solution was allowed to warm to room temperature. Exposure of this solution to N_2O, with vigorous stirring, caused a gradual color change from orange to green over the course of less than 1 h, concomitant with the formation of a brown precipitate. The mixture was allowed to stir for a total of 4 h. After evaporation of solvent under reduced pressure, a green-and-tan residue was obtained. Extraction of this residue into C_6D_6 and filtration through a plug of Celite afforded a dark green solution. ^{1}H NMR (500 MHz, C_6D_6): δ 7.73−7.79 (m, $OPPh_3$), 7.36−7.43 (m, PPh_3), 6.96−7.07 (m, overlapping PPh_3 and $OPPh_3$), 6.77 (s, 4H, m-CH), 6.06 (s, 2H, NCH), 5.92 (s, Cp), 2.12 (s, 6H, p-CH_3), 1.98 (s, 12H, o-CH_3). ^{31}P{^{1}H} NMR (500 MHz, C_6D_6): δ 23.4 (s, $OPPh_3$), −6.5 (s, PPh_3).

Reaction between N_2O and 1a Followed by PPh_3 Addition. A Schlenk flask with a stir bar was charged with **1a** (0.100 g, 0.183 mmol) and THF (15 mL) under an atmosphere of nitrogen, producing an orange solution. Three freeze−pump−thaw cycles were performed, after which the solution was allowed to warm to room temperature. Exposure of this solution to N_2O, with vigorous stirring, caused the formation of a brown precipitate. The mixture was allowed to stir for a total of 4 h. After evaporation of solvent under reduced pressure, a tan residue was obtained. Triphenylphosphine (0.144 g, 0.549 mmol) and THF (15 mL) were added to the flask, and the resulting mixture was allowed to stir for an additional 3 h. Solvent was again evaporated under reduced pressure, and extraction of the resulting tan residue into C_6D_6 and filtration through a plug of Celite afforded an orange solution. ^{1}H NMR (500 MHz, C_6D_6): δ 7.36−7.43 (m, PPh_3), 7.00−7.07 (m, PPh_3), 6.78 (s, 4H, m-CH), 6.04 (s, 2H,

dx.doi.org/10.1021/ic501054z | Inorg. Chem. 2014, 53, 7730−7737

NCH), 5.91 (s, Cp), 2.13 (s, 6H, *p*-CH_3), 1.98 (s, 12H, *o*-CH_3). $^{31}P\{^1H\}$ NMR (500 MHz, C_6D_6): δ −6.7 (s, PPh_3).

Headspace Analysis of Reaction between N_2O and ***1a*** *in the Presence of PPh_3.* A Schlenk flask with a stir bar was charged with **1a** (0.100 g, 0.183 mmol), triphenylphosphine (0.144 g, 0.551 mmol), and THF (56 mL) under an atmosphere of nitrogen, producing a yellow solution with a headspace volume approximately equal to 5 equiv of gas, assuming ideal behavior at 298 K. The flask was sealed with a rubber septum. Three freeze−pump−thaw cycles were performed, after which the solution was allowed to warm to room temperature. Exposure of this solution to N_2O, with vigorous stirring, caused the formation of a brown precipitate. The mixture was allowed to stir for a total of 4 h. A mass spectrum of the headspace after the reaction was obtained via 2 μL injections at 40 °C.

Competition between PPh_3 and P(p-tolyl)$_3$ in Reaction between N_2O and ***1a.*** A Schlenk flask with a stir bar was charged with **1a** (0.0100 g, 0.0184 mmol), 1-$^1/_2$ equiv of triphenylphosphine (0.0072 g, 0.0275 mmol), 1-$^1/_2$ equiv equivalents of tri-*p*-tolylphosphine (0.0084 g, 0.0275 mmol) and THF (5 mL) under an atmosphere of nitrogen, producing a yellow solution. Three freeze−pump−thaw cycles were performed, after which the solution was allowed to warm to room temperature. Exposure of this solution to excess N_2O, with vigorous stirring, caused a gradual color change from yellow to green-brown over the course of less than 1 h, concomitant with the formation of a brown precipitate. The mixture was allowed to stir for a total of 24 h. After evaporation of solvent under reduced pressure, a tan residue was obtained. Extraction of this residue into C_6D_6 and filtration through a plug of Celite afforded a yellow-green solution. $^{31}P\{^1H\}$ NMR (400 MHz, C_6D_6): δ 23.39 (s, P(*p*-tol)$_3$O), 23.29 (s, PPh_3O), −6.68 (s, PPh_3), −8.91 (s, P(*p*-tol)$_3$).

Competition between P(o-tolyl)$_3$ and P(p-tolyl)$_3$ in Reaction between N_2O and ***1a.*** A Schlenk flask with a stir bar was charged with **1a** (0.0100 g, 0.0184 mmol), 1-$^1/_2$ equiv of tri*o*-tolylphosphine (0.0084 g, 0.0275 mmol), 1-$^1/_2$ equiv of tri-*p*-tolylphosphine (0.0084 g, 0.0275 mmol) and THF (5 mL) under an atmosphere of nitrogen, producing a yellow solution. Three freeze−pump−thaw cycles were performed, after which the solution was allowed to warm to room temperature. Exposure of this solution to excess N_2O, with vigorous stirring, caused a gradual color change from yellow to brown over the course of less than 1 h, concomitant with the formation of a brown precipitate. The mixture was allowed to stir for a total of 24 h. After evaporation of solvent under reduced pressure, a tan residue was obtained. Extraction of this residue into C_6D_6 and filtration through a plug of Celite afforded a yellow solution. $^{31}P\{^1H\}$ NMR (400 MHz, C_6D_6): δ 23.40 (s, P(*p*-tol)$_3$O), −9.24 (bs, P(*p*-tol)$_3$), −31.13 (s, P(*o*-tol)$_3$).

■ ASSOCIATED CONTENT

Ⓢ Supporting Information

Spectroscopic characterization, crystallographic data. This material is available free of charge via the Internet at http://pubs.acs.org.

■ AUTHOR INFORMATION

Corresponding Author

*E-mail: npm@uic.edu.

Notes

The authors declare no competing financial interest.

■ ACKNOWLEDGMENTS

This research was supported by start-up funds from the Department of Chemistry at the University of Illinois at Chicago (UIC), and by a Pilot Grant from the Campus Research Board at UIC. X-ray crystallography data for **2a**, **2b**, and **3** were collected at the X-ray Structural Laboratory at Marquette University (Milwaukee, WI) by Dr. Sergey Lindeman. X-ray energy dispersive spectra and GC-MS data were collected at the Research Resources Center at UIC by Drs. Alan Nicholls and John (Art) Anderson, respectively.

■ ABBREVIATIONS

CODH, carbon monoxide dehydrogenase; Cp, η^5-cyclopentadienyl; Cp*, η^5-pentamethylcyclopentadienyl; Fp, $FeCp(CO)_2$; Fp*, $FeCp^*(CO)_2$; IMes, *N*,*N*′-bis(2,4,6-trimethylphenyl)imidazol-2-ylidene; IPr, *N*,*N*′-bis(2,6-diisopropylphenyl)imidazol-2-ylidene; N_2OR, nitrous oxide reductase; NHC, *N*-heterocyclic carbene; ZSM, Zeolite Secony Mobil

■ REFERENCES

(1) Recent reviews: (a) Tsuji, Y.; Fujihara, T. *Chem. Commun.* **2012**, *48*, 9956−9964. (b) Olah, G. A.; Goeppert, A.; Prakash, G. K. S. *J. Org. Chem.* **2009**, *74*, 487−498. (c) Wang, W.; Wang, S.; Ma, X.; Gong, J. *Chem. Soc. Rev.* **2011**, *40*, 3703−3727.

(2) van der Vlugt, J. I. *Eur. J. Inorg. Chem.* **2012**, 363−375.

(3) Jeoung, J. H.; Dobbek, H. *Science* **2007**, *318*, 1461−1464.

(4) Pauleta, S. R.; Dell'Acqua, S.; Moura, I. *Coord. Chem. Rev.* **2011**, *257*, 332−349.

(5) Piro, N. A.; Lichterman, M. F.; Harman, W. H.; Chang, C. J. *J. Am. Chem. Soc.* **2011**, *133*, 2108−2111.

(6) Gorelsky, S. I.; Ghosh, S.; Solomon, E. I. *J. Am. Chem. Soc.* **2006**, *128*, 278−290.

(7) (a) Tsai, M.-L.; Hadt, R. G.; Vanelderen, P.; Sels, B. F.; Schoonheydt, R. A.; Solomon, E. I. *J. Am. Chem. Soc.* **2014**, *136*, 3522−3529. (b) Smeets, P. J.; Hadt, R. G.; Woertink, J. S.; Vanelderen, P.; Schoonheydt, R. A.; Sels, B. F.; Solomon, E. I. *J. Am. Chem. Soc.* **2010**, *132*, 14736−14738.

(8) Selected references: (a) Krogman, J. P.; Foxman, B. M.; Thomas, C. M. *J. Am. Chem. Soc.* **2011**, *133*, 14582−14585. (b) Memmler, H.; Kauper, U.; Schneider, A.; Fabre, S.; Bezougli, I.; Lutz, M.; Galka, C.; Scowen, I. J.; Mcpartlin, M.; Gade, L. H. *Chem.—Eur. J.* **2000**, *6*, 692−708. (c) Hanna, T. A.; Baranger, A. M.; Bergman, R. G. *J. Am. Chem. Soc.* **1995**, *117*, 11363−11364.

(9) Selected references: (a) Fachinetti, G.; Zanazzi, P. F.; Floriani, C. *J. Am. Chem. Soc.* **1978**, *100*, 7405−7407. (b) Bianchini, C.; Meli, A. *J. Am. Chem. Soc.* **1984**, *106*, 2698−2699. (c) Mömming, C. M.; Otten, E.; Kehr, G.; Fröhlich, R.; Grimme, S.; Stephan, D. W.; Erker, G. *Angew. Chem., Int. Ed.* **2009**, *48*, 6643−6643. (d) Otten, E.; Neu, R. C.; Stephan, D. W. *J. Am. Chem. Soc.* **2009**, *131*, 9918−9919. (e) Tskhovrebov, A. G.; Vuichoud, B.; Solari, E.; Scopelliti, R.; Severin, K. *J. Am. Chem. Soc.* **2013**, *135*, 9486−9492.

(10) Selected examples: (a) Uyeda, C.; Peters, J. C. *J. Am. Chem. Soc.* **2013**, *135*, 12023−12031. (b) Cooper, B. G.; Napoline, J. W.; Thomas, C. M. *Catal. Rev.* **2012**, *54*, 1−40. (c) Berkefeld, A.; Piers, W. E.; Parvez, M. *J. Am. Chem. Soc.* **2010**, *132*, 10660−10661.

(11) Recent references: (a) Courtemanche, M.-A.; Légaré, M.-A.; Maron, L.; Fontaine, F.-G. *J. Am. Chem. Soc.* **2013**, *135*, 9326−9329. (b) Piers, W.; Berkefeld, A.; Parvez, M.; Castro, L.; Maron, L.; Eisenstein, O. *Chem. Sci.* **2013**, *4*, 2152−2162. (c) Shintani, R.; Nozaki, K. *Organometallics* **2013**, *32*, 2459−2462.

(12) Recent references: (a) Bauer, J.; Braunschweig, H.; Damme, A.; Radacki, K. *Angew. Chem., Int. Ed.* **2012**, *51*, 10030−10033. (b) Bauer, J.; Braunschweig, H.; Dewhurst, R. D. *Chem. Rev.* **2012**, *112*, 4329−4346. (c) Ma, M.; Sidiropoulos, A.; Ralte, L.; Stasch, A.; Jones, C. *Chem. Commun.* **2013**, *49*, 48−50.

(13) Jayarathne, U.; Mazzacano, T. J.; Bagherzadeh, S.; Mankad, N. P. *Organometallics* **2013**, *32*, 3986−3992.

(14) Mazzacano, T. J.; Mankad, N. P. *J. Am. Chem. Soc.* **2013**, *135*, 17258−17261.

(15) van der Sluys, L. S.; Miller, M. M.; Kubas, G. J.; Caulton, K. G. *J. Am. Chem. Soc.* **1991**, *113*, 2513−2520.

(16) Baird, M. C.; Wilkinson, G. *Chem. Commun.* **1966**, 514−515.

(17) Recent examples: (a) Bheemaraju, A.; Beattie, J. W.; Lord, R. L.; Martin, P. D.; Groysman, S. *Chem. Commun.* **2012**, *48*, 9595−9597.

(b) Haack, P.; Limberg, C.; Tietz, T.; Metzinger, R. *Chem. Commun.* **2011**, *47*, 6374−6376.
(18) Selected references: (a) Ellis, J. E.; Fennell, R. W.; Flom, E. A. *Inorg. Chem.* **1976**, *15*, 2031−2036. (b) Pinkes, J. R.; Tetrick, S. M.; Landrum, B. E.; Cutler, A. R. *J. Organomet. Chem.* **1998**, *566*, 1−7. (c) Bianchini, C.; Mealli, C.; Meli, A.; Orandini, A.; Sacconi, L. *Inorg. Chem.* **1980**, *19*, 2968−2975. (d) Southern, T. G.; Oehmichen, U.; Marouille, J. Y. L.; Bozec, H. L.; Grandjean, D.; Dixneuf, P. H. *Inorg. Chem.* **1980**, *19*, 2976−2980.
(19) Gibson, D. H. *Chem. Rev.* **1996**, *96*, 2063−2096.
(20) (a) Hou, Z.; Zhang, L. *Chem. Sci.* **2013**, *4*, 3395−3403. (b) Mankad, N. P.; Gray, T. G.; Laitar, D. S.; Sadighi, J. P. *Organometallics* **2004**, *23*, 1191−1193. (c) Shintani, R.; Nozaki, K. *Organometallics* **2013**, *32*, 2459−2462. (d) Laitar, D. S.; Müller, P.; Sadighi, J. P. *J. Am. Chem. Soc.* **2005**, *127*, 17196−17197. (e) Bhattacharyya, K. X.; Akana, J. A.; Laitar, D. S.; Berlin, J. M.; Sadighi, J. P. *Organometallics* **2008**, *27*, 2682−2684.
(21) Lee, G. R.; Cooper, N. J. *Organometallics* **2001**, *4*, 794−797.
(22) Selected references: (a) Chadeayne, A. R.; Wolczanski, P. T.; Lobkovsky, E. B. *Inorg. Chem.* **2004**, *43*, 3421−3432. (b) Baranger, A. M.; Hanna, T. A.; Bergman, R. G. *J. Am. Chem. Soc.* **1995**, *117*, 10041−10046. (c) Laplaza, C. E.; Odom, A. L.; Davis, W. M.; Cummins, C. C.; Protasiewicz, J. D. *J. Am. Chem. Soc.* **1995**, *117*, 4999−5000. (d) Vaughan, G. A.; Hillhouse, G. L.; Rheingold, A. L. *J. Am. Chem. Soc.* **1990**, *112*, 7994−8001.
(23) (a) Whited, M. T.; Grubbs, R. H. *J. Am. Chem. Soc.* **2008**, *130*, 16476−16477. (b) Ménard, G.; Hatnean, J. A.; Cowley, H. J.; Lough, A. J.; Rawson, J. M.; Stephan, D. W. *J. Am. Chem. Soc.* **2013**, *135*, 6446−6449. (c) Tskhovrebov, A. G.; Solari, E.; Scopelliti, R.; Severin, K. *Organometallics* **2012**, *31*, 7235−7240. (d) Neu, R. C.; Otten, E.; Lough, A.; Stephan, D. W. *Chem. Sci.* **2011**, *2*, 170−176.
(24) (a) Bar-Nahum, I.; Gupta, A. K.; Huber, S. M.; Ertem, M. Z.; Cramer, C. J.; Tolman, W. B. *J. Am. Chem. Soc.* **2009**, *131*, 2812−2814. (b) Kiefer, G.; Jeanbourquin, L.; Severin, K. *Angew. Chem., Int. Ed.* **2013**, *52*, 6302−6305.
(25) Ren, H.; Zhao, X.; Xu, S.; Song, H.; Wang, B. *J. Organomet. Chem.* **2006**, *691*, 4109−40113.
(26) (a) Roman, J. S.; Groves, J. T. *J. Am. Chem. Soc.* **1995**, *117*, 5594−5595. (b) Yamamoto, A.; Kitazume, S.; Pu, L. S.; Ikeda, S. *J. Am. Chem. Soc.* **1971**, *93*, 371−380. (c) Leont'ev, A. V.; Tomilova, L. G.; Fomicheva, A. O.; Proskurina, M. V.; Zefirov, N. S. *Russ. J. Gen. Chem.* **2001**, *71*, 648−649. (d) Chernysheva, A. N.; Beloglazkina, E. K.; Moiseeva, A. A.; Antipin, R. L.; Zyk, N. V.; Zefirov, N. S. *Mendeleev Commun.* **2012**, *22*, 70−72. (e) Tanaka, H.; Hashimoto, K.; Suzuki, K.; Kitaichi, Y.; Sato, M.; Ikeno, T.; Yamada, T. *Bull. Chem. Soc. Jpn.* **2004**, *77*, 1905−1914. (f) Yamada, T.; Suzuki, K.; Hashimoto, K.; Ikeno, T. *Chem. Lett.* **1999**, 1043−1044. (g) Arzoumanian, H.; Nuel, D.; Sanchez, J. *J. Mol. Catal.* **1991**, *63*, L9−L11.
(27) Poh, S.; Hernandez, R.; Inagaki, M.; Jessop, P. G. *Org. Lett.* **1999**, *1*, 583−586.
(28) Armarego, W. L. F.; Chai, C. C. L. *Purification of Laboratory Chemicals*, 6th ed.; Butterworth-Heinemann: Burlington, MA, 2009.
(29) (a) Jafarpour, L.; Stevens, E. D.; Nolan, S. P. *J. Organomet. Chem.* **2000**, *606*, 49−54. (b) Arduengo, A. J., III; Krafczyk, R.; Schmutzler, R.; Craig, H. A.; Goerlich, J. R.; Marshall, W. J.; Unverzagt, M. *Tetrahedron* **1999**, *55*, 14523−14534. (c) Hintermann, L. *Beilstein J. Org. Chem.* **2007**, *3*, 22.
(30) (a) Santoro, O.; Collado, A.; Slawin, A. M. Z.; Nolan, S. P.; Cazin, C. S. J. *J. Chem. Soc., Chem. Comm.* **2013**, *49*, 10483−10485. (b) Kaur, H.; Zinn, F. K.; Stevens, E. D.; Nolan, S. P. *Organometallics* **2004**, *23*, 1157−1160.
(31) Guerchaisa, V.; Astruc, D. *J. Chem. Soc., Chem. Comm.* **1985**, 835−837.
(32) Sheldrick, G. M. *Acta Crystallogr.* **2008**, *A64*, 112−122.